ISSN: 0975-8585

Research Journal of Pharmaceutical, Biological and Chemical Sciences

Molecular Mobility in Copolymers of Vinylidene Fluoride with Tetrafluoroethylene and The Influence of Cold Drawing.

Lyana O. Shoranova*, Sergey A. Bondarenko, Andrey E. Afonkin, Eugene V. Luchkin, and Anastasia S. Gadlevskaya.

Joint Stock Company «Federal State Research and Design Institute of Rare Metal Industry» (Institute «GIREDMET»), 119017, Moscow, Russian Federation.

ABSTRACT

As in isotropic samples (cold stretched films) by the method of dielectric relaxation revealed that there are two types of mobility, one of which is associated with the cooperative movement, and the other with local. At low multiplicities of drawing observed anomalous behavior of the activation parameters. This has been attributed to incomplete restructuring laminarnykh crystals. At high frequency cold-drawing the formed crystals with maloprotochnyh transverse dimensions. Also discovered the presence of anisotropic amorphous phase with higher packing of the chains. This affects the characteristics of the activation parameters of the observed relaxation processes. Analyzes the behavior of acoustic modules under mechanical loading cold-extruded films. Change the marked module associated with the transition of anisotropic amorphous phase in the crystal. A comparison of the values of the residual polarization in an isotropic and cold-extruded films.

Keywords: vinylidene fluoride, tetrafluoroethylene, copolymers, relaxation, electric hysteresis, ferroelectric films.

Corresponding author

ISSN: 0975-8585

INTRODUCTION

PVDF is a convenient model subject for studying the molecular dynamics in crystallizable polymers. In this case, a high dipole moment of its monomer unit allows the technique of dielectric spectroscopy to be used for this purpose. Furthermore, the choice of PVDF as a subject of study is also due to its ferroelectric properties [1–3], wherein the character of chain dynamics in the disordered phase has a strong effect on these parameters [3]. The investigation of the molecular mobility and ferroelectricity in uniaxially drawn films seems to be important because, in this case, orientation is accompanied by an increase in residual polarization [2, 3]. The residual polarization is responsible for all piezoelectric and pyroelectric coefficients [3] and, thus, may provide higher output parameters of sensors based on the above materials [4, 5].

In this work, we studied the molecular mobility in the glass transition region for some oriented films of the vinylidene fluoride (VDF)–tetrafluoroethylene (TFE) copolymer, which immediately crystallize in the ferroelectric β-phase from their isotropic state [6]. In this connection, the orientation of a film is not aggravated by any solid-state transformations in the crystal lattice. This situation should lead to the development of a simpler structure of the polymer in its oriented state, thus enabling the experimental data to be unequivocally interpreted.

EXPERIMENTAL

The test films were prepared from the VDF–TFE (94 : 6) copolymer containing 4.5 mol % of "head-totail" defects [7]. For orientation, the initial isotropic films were obtained by nonisothermic crystallization from melt and quenching in water at room temperature. The films were oriented at 20°C by uniaxial tensile drawing (with necking) to different draw ratios λ, which were assessed as the length of the deformed films between the clamps. The morphology of the initial films was studied by the technique of small-angle polarized light scattering. The analysis shows that the isotropic films are characterized by the presence of structures similar to optically anisotropic rod aggregates [8] or small-sized and highly imperfect spherulites [9]. Cold drawing was performed using an Instron1122 tensile machine at a pulling rate of 10 mm/min, with recording of the acting mechanical stress [10]. After drawing and unloading, the oriented films were characterized by the shrinkage $S = \frac{\lambda - \lambda_m}{\lambda}$, where λ and λ_m stand for the draw ratios estimated from the distance between the clamps and from the position of ink marks upon unloading. The mean orientation of the oriented films was characterized by the birefringence Δn, which was determined with a Berec compensator. The morphology of the oriented films was studied by the smallangle X-ray scattering technique [10]. The longitudinal and lateral dimensions of the crystallites in the oriented films were estimated using the Scherrer–Debye equations for the (001), (200), and (110) X-ray reflections, respectively. The conformational state of chains in the drawn films was studied using IR spectroscopy. The measurements were performed in polarized light. The optical density D and dichroic ratio R were calculated from the following relationships: $D = D_{||} + 2D_{\perp}/3$ and $R = D_{||}/D_{\perp}$, where $D_{||}$ and $D_{\perp}$ are the optical densities at the corresponding absorption bands with the polarization vector directed along and perpendicular to the direction of tensile drawing, respectively.

The process of uniaxial drawing was also monitored using the ultrasonic pulse technique at a frequency of 200 kHz [11]. The acoustic pulse source was located on the side of one clamp of the deformed film, whereas the sonic-signal sensor was mounted near the other clamp; as a result, the speed of sound was measured along the direction of tensile drawing of the film. The oriented films were also characterized by the extent of irreversible increase in the free volume. The free-volume fraction was calculated through the following relationship [8]: $\frac{\Delta V}{V} = \frac{ls - l_0 s_0}{l_0 s_0}$, where l_0 and s_0 are, respectively, the length and cross sectional area of the initial film before tensile drawing and l and s are the same parameters after tensile drawing and unloading.

To study the dielectric properties, aluminum electrodes 0.1 μm in thickness were deposited on the film surface. The temperature–frequency dependences of dielectric permittivity ε' and dielectric loss ε'' were measured with a TR-9701 instrument over the frequency range of 60 Hz–100 kHz in the isothermal mode. The accuracy of temperature control was 0.5°. The components of dielectric permittivity were presented on the complex ε''–ε' plane. The as-obtained dependences allow one to estimate both static ε_0 and high-frequency

ISSN: 0975-8585

dielectric permittivity ε_∞. The procedure for calculating the activation parameters was described earlier [12]. Hysteresis curves were obtained at room temperature on a Sawyer–Tower device powered by a 50-Hz ac voltage.

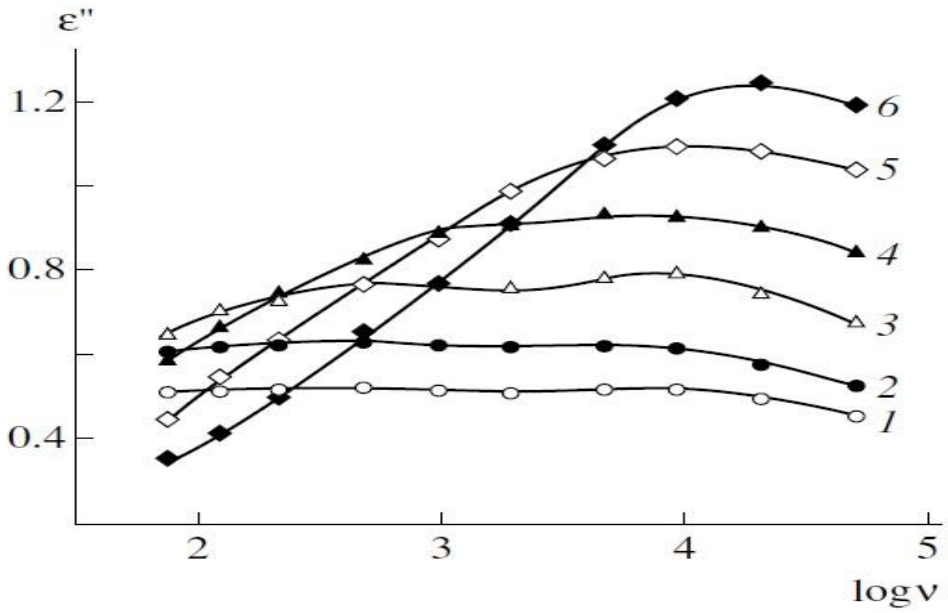

Fig. 1. Frequency dependences of the dielectric loss factor in cold-drawn VDF–TFE copolymer film with λ = 4 at (*1*) –43, (*2*) –38, (*3*) –33, (*4*) –28, (*5*) –23, and (*6*) –17 °C.

RESULTS AND DISCUSSION

For the films under study, the isochronous curves of ε'' appear to be qualitatively similar to those for the isotropic samples. The coincidence of the low-temperature branches of the curves at different frequencies of the applied electric field indicates the occurrence of two overlapping processes (Fig. 1). Table 1 presents the activation parameters of both relaxation processes in the isotropic and oriented samples, which were calculated from the isochronous dependences of the loss factor [12, 13].

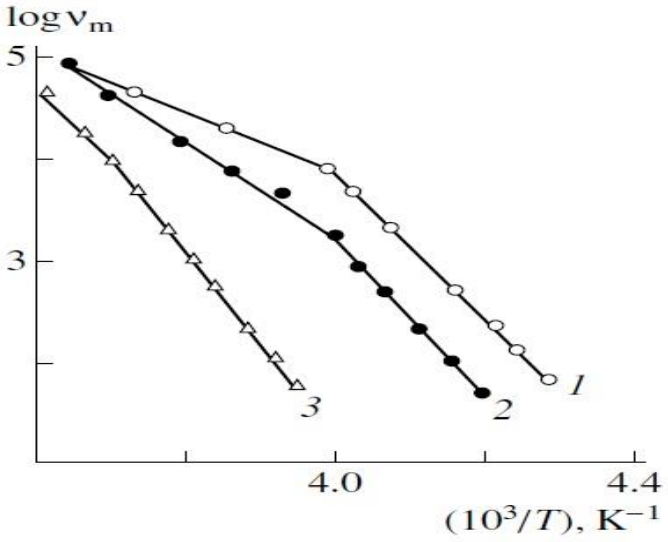

Fig. 2. Transition maps for the cold-drawn VDF–TFE copolymer films with = (*1*) 2, (*2*) 4, and (*3*) 6.

ISSN: 0975-8585

As follows from Fig. 2, the transition maps of colddrawn specimens (as well as the isotropic films) are characterized by the presence of two Arrhenius straight lines with a characteristic bending point. The low-temperature part of the plots refers to the manifestation of α_a-relaxation, which is due to the micro-Brownian motion in the disordered regions. The high-temperature part of the linear plots is associated with the occurrence of the combined (α_a-β)-relaxation process when the corresponding relaxation times appear to be comparable, and distinguishing between such processes by experimental means becomes impossible (curves 4 and 5 in Fig. 1) [12, 13].

Table 1. Relaxation parameters for isotropic and cold-drawn VDF–TFE copolymer films

λ	$\Delta n \times 10^{-3}$	T_g, °C	ΔE	ΔH	ΔS, e.u.	T_β, °C	ΔE	ΔH	ΔS, e.u.
			kJ/mol			kJ/mol			
		α_a-relaxation				(α_a-β)-relaxation			
1	-	-50	172	169	535	-76	63	61	86
2	12,8	-53	138	136	395	-86	58	56	77
4	30,0	-42	162	160	446	-62	86	84	173
6	32,6	-30	191	189	550	-34	157	155	420

As follows from Table 1, as compared with the isotropic sample, the oriented sample with a draw ratio of λ = 2 has a hindered mobility. This tendency is displayed as a noticeable decrease in the freezing-out temperature of both modes of molecular mobility, as well as in the values of their activation parameters. This behavior is explained by the specific features of "disassembling" (melting) of initial lamellar crystals [14] upon cold drawing. The low temperature of uniaxial orientation impedes the process of subsequent recrystallization of the amorphous-phase chains formed. In the case of quick unloading of the deformed polymer (as in our experiments), a higher proportion of the disordered phase should be expected. This conclusion follows from the dielectric data. Figure 3 shows the temperature dependence for the dielectric permittivity .' of the initial film and the film after its cold drawing up to λ = 2. First, the α_a-relaxation region in the oriented sample is seen to be shifted to lower temperatures, as has been noted above. Second, at room temperature, ε' of the film with λ = 2 is higher than that of the isotropic sample. Since the dielectric permittivity of the amorphous phase under these conditions is several times higher than ε' of the crystal [3], this trend may be explained by an increased relative amount of chains in the disordered phase.

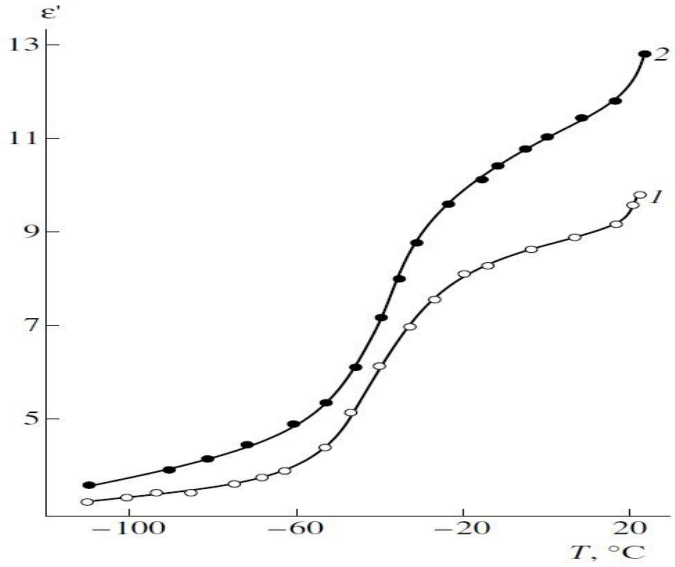

Fig. 3. The temperature dependences of dielectric permittivity in (*1*) isotropic and (*2*) cold-drawn (up to λ = 2) copolymer film. ν = 60 Hz.

Once the modulus of the crystalline phase at the drawing temperature is an order of magnitude higher than that of the amorphous phase [6], increments in the amorphous phase can be detected by the acoustic technique. Figure 4 shows changes in the speed of sound along the drawing axis during orientation of

the test film. It is seen that the speed of sound decreases in the region preceding the neck formation. This fact may be associated with further amorphization (along the draw axis) of the deformed sample. This behavior is common for crystallizable polymers, as an increase in the proportion of high-mobility kinetic units has been also observed with the NMR technique at the stage of necking upon the tensile drawing of nylon-6 [15]. The aforementioned additional amorphization seems to be accompanied by a qualitative change in the microstructure of the disordered phase. A similar decrease in the speed of sound observed upon the tensile drawing of amorphous PMMA [16] suggests that, at early stages, tensile drawing leads to a decrease in the packing density of chains in the disordered phase. As applied to crystallizable polymers, these speculations are proved by the electron microscopy data [14, 17] and positron annihilation lifetime spectra [18].

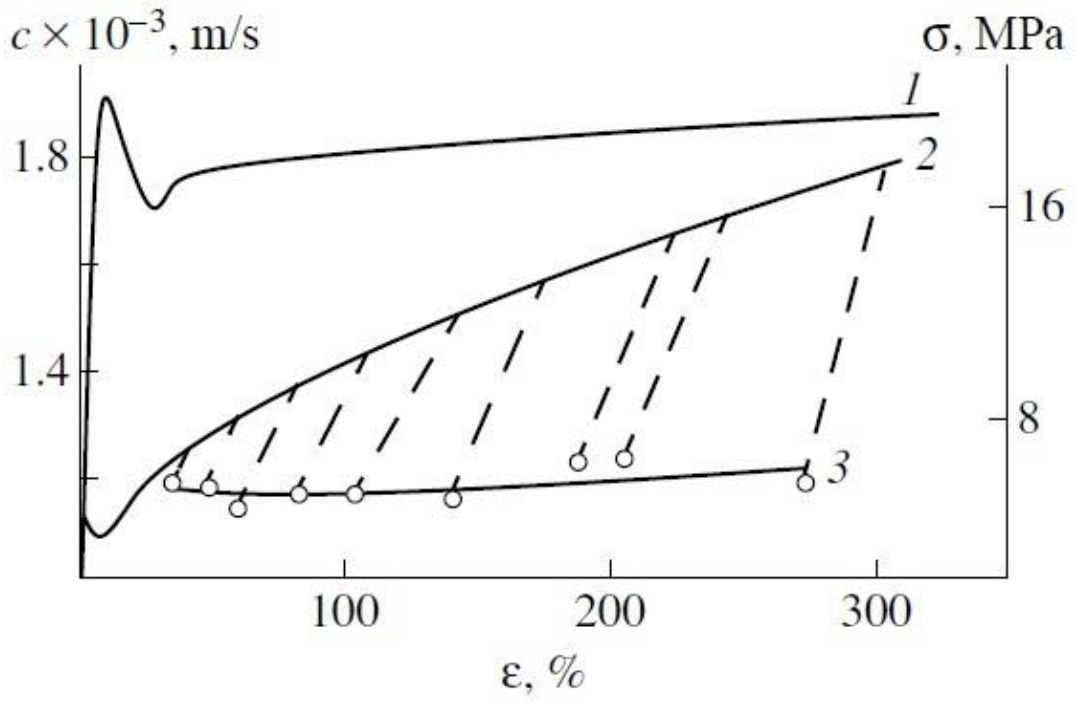

Fig. 4. (*1*) Mechanical stress and (*2*, *3*) lateral speed of sound vs. relative tensile strain upon the cold drawing of VDF–TFE copolymer films. Curves *2* and *3* correspond to the speed of sound in the loaded and unloaded sample states, respectively.

In this connection, the changes in the dielectric and acoustic characteristics of the samples with low draw ratios (Figs. 3, 4) should be associated not only with an increase in the volume fraction of the disordered phase but also with a decrease in its packing density. This effect results in the alteration of relaxation parameters for the α_a-process. As follows from Table 1, on passing from the isotropic sample to the oriented sample with λ = 2, the entropy and enthalpy of activation decrease by 26 and 20%, respectively. Substantial facilitation of cooperative mobility in the amorphous phase should enhance the mobility of both electrode-injected and intrinsic (or extrinsic) charge carriers. For the conductivity of a polymer dielectric at high field strengths, this situation corresponds to a higher current density. In terms of the thermal mechanism of electric breakdown, one may expect lower values of breakdown voltage. Indeed, according to our data, the breakdown field strength for the isotropic films is equal to 1 MV/cm, whereas it decreases down to 400 kV/cm in the film with λ = 2.

ISSN: 0975-8585

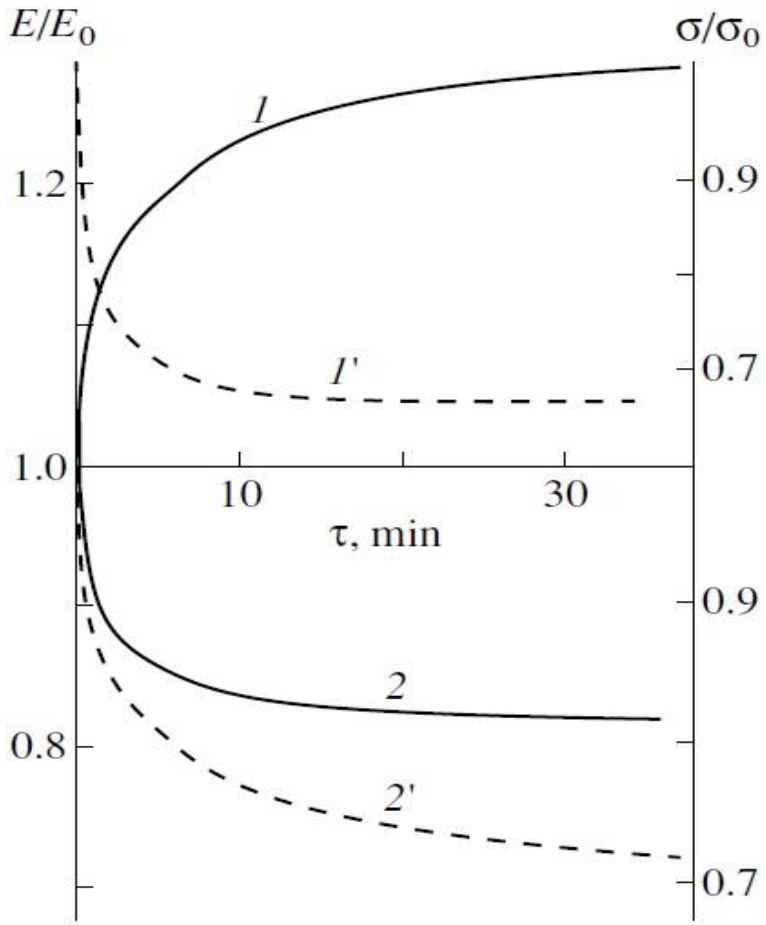

Fig. 5. (*1*, *2*) Kinetic curves of changes in the longitudinal speed of sound and (*1*', *2*') applied mechanical stress at a relative tensile strain of = (*1*, *1*') 8 and (*2*, *2*') 400%. T_d = 70°C.

It might seem that the microstructure of the disordered phase in the case under consideration is metastable. Figure 5 shows the kinetic curves of the longitudinal speed of sound along the draw direction for the copolymer films with two different relative strains ε. As is seen, in both cases, the stress relaxation is accompanied by structural changes which lead to quite different manners of behavior of the acoustic modulus. At ε = 8% (the region of minimum in curve 2, Fig. 4), the modulus increases with time, whereas its value decreases at high draw ratios (curve 2, Fig. 5). For the specimens with low tensile strains, this increase in the acoustic modulus obviously reflects the transformation of the aforementioned metastable state to that closer to equilibrium. This transition can be due to the collapse (healing) of microcrazes [17] and to the fact that some chains in the amorphous phase become closer to each other upon the formation of fibrillar crystals. As follows from Fig. 5, the "recovery" process of the acoustic modulus (the transition to more equilibrium fibrillar crystals) takes tens of minutes even at 70°C. At the draw temperature (20°C in the given case), the kinetics of this process should be far more hindered. The rapid unloading of samples with low λ will partially fix the structure of the transition state, and it is this structure that will be responsible of the above-noted change in the molecular dynamics in amorphous regions.

Let us turn back to Fig. 2. As is seen, an increase in the draw ratio of the oriented films is accompanied by a consistent increase in hindrance to both cooperative α_a-process and more localized β-process. This conclusion follows from an evident decrease (at the same temperature) in the mean frequency ν of reorientation of kinetic units. If ν is assumed to be proportional to the local free volume fraction, this means that increasing the draw ratio increases the chain packing density in noncrystallizable regions. This process may be provided by a decrease in the degree of folding of the formed fibrillar crystals, as was theoretically predicted for flexible-chain polymers [19]. Experimental evidence of this decrease can be obtained using a spectroscopic technique. If the chain fold regions are formed by segments in helical conformation, a decrease

in the degree of crystal folding will be accompanied by an increase in the proportion of isomers in the all-trans conformation in the amorphous phase. For PVDF and related copolymers, an absorption band at 470 cm^{-1} corresponds to this conformation of chains [6]. Table 2 presents variations in the parameters of this band with increasing the draw ratio of test samples from 4 to 6. It is seen that the normalized intensity considerably increases. The enhancement in intensity implies that this increase in the draw ratio increases the proportion of all-trans conformations in the amorphous by more than a factor of 2. In this case, the dichroic ratio R of the 470-cm^{-1} absorption band also markedly increases.

The appearance of segments with preferable arrangement of their axes with respect to the draw direction in the amorphous phase is equivalent to the appearance of regions of the anisotropic amorphous phase. Their presence can also be proved by the X-ray diffraction data. As follows from Fig. 6, upon scanning along the equator, the angular position of the amorphous halo is shifted to larger angles (the dashed line in the curve) as compared with the scanning in the meridional direction. This implies that part of the chains in the amorphous phase (so-called anisotropic amorphous phase [20, 21]) aligned with the draw axis has a higher packing density.

These transformations in the microstructure of the amorphous phase upon cold drawing have different effects on the characteristics of the two relaxation processes. For the α_a-process, ΔH and ΔS increase by tens of percent, whereas this increase for the (α_a-β)-process is as great as hundreds of percent (Table 1). If an increase in the draw ratio is supposed to provide an increase in the proportion of the anisotropic amorphous phase with a higher packing density, the (.a -.)-relaxation process should be related to the relaxation in the above regions.

The longitudinal and lateral dimensions of the crystals were calculated from the width of the meridional (001) reflection and basic intermolecular (200, 110) reflection of the β-phase, respectively (Fig. 6); the results are summarized in Table 2. For the sake of comparison, Table 2 presents the same parameters for films oriented at high draw temperatures T_d. As is seen, the parameters of the test samples obtained via cold drawing are much higher than those of the samples oriented at high T_d. Small-angle X-ray diffraction patterns show that the character of orientation appears to be quite different in both cases. For the sample with T_d = 120°C, the diagram shows a two-stroke diffraction pattern, whereas four strokes are seen in the case of the colddrawn sample.

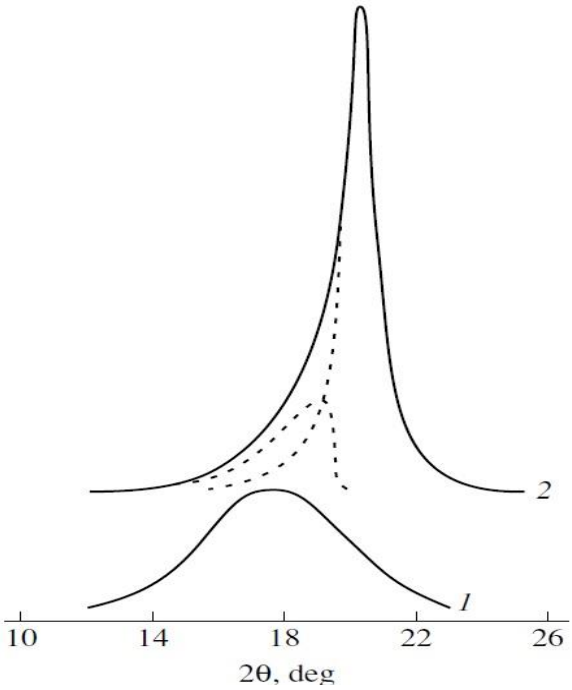

Fig. 6. The X-ray diffraction curves for the VDF–TFE copolymer specimens prepared by uniaxial tensile drawing to a draw ratio of λ = 6 at 20°C. The angle between the direction of recording and draw axis is equal to (*1*) 0° (meridian) and (*2*) 90° (equator). See the text for comments.

According to model calculations [22], this finding may be rationalized as follows. At high draw temperatures, well-developed lamellar crystals are formed. Their lateral size ($l_{110,\ 200}$) is large (Table 2). In contrast, this parameter appears to be two times lower for the cold-drawn sample. The longitudinal size l_{001} of the crystals also appears to be much lower. According to the conclusions made in [22], the four-stroke pattern suggests that small-sized crystallites are skewed. This shape may be due to increased external stress upon tensile drawing [10] and the impossibility of its relaxation at low temperatures. In the case of the cold-drawn samples, the intensity of the small-angle meridional reflection appears to be much lower [10]. As this intensity is proportional to the difference in densities $(\Delta\rho)^2$ of the two phases along the draw direction, a decrease in $(\Delta\rho)^2$ in cold-drawn films could be explained by an increased content of the mesomorphic (more densely packed) component of the amorphous phase. Therefore, the small-angle X-ray scattering data and wide-angle X-ray diffractograms (Fig. 6) suggest the following conclusion: as the draw ratio increases, the relative amount of the anisotropic amorphous phase with a high packing density increases.

Table 2. Structural characteristics of oriented VDF–TFE copolymer films

T_d, °C	λ	Orientation type	L, nm	l_{001}	$l_{110,200}$	$\Delta\phi_{001}$	$\Delta\phi_{110,200}$	f_c	$(D/d)_{470}$, cm^{-1}	R_{470}
20	4	-							82	2.1
	6	°	8.8	4.9	6.2	18	20	0.86	179	4.9
		- -								
120		-								
	6	°	12.1	7.1	12.7	14	16	0.91	66	3.2
		-								

Table 2 shows the smearing angles Δϕ of the most characteristic reflections, which were obtained by azimuthal scanning. From these data, orientation functions f_c for the crystal were calculated (from the (001) X-ray reflection). In the case of cold drawing, the crystals are seen to be characterized by a lower orientation function as compared with that obtained using high-temperature orientation, which may be associated with the abovementioned lack of conditions for the relaxation of amorphous-phase chains. The films studied have a smaller long period L, i.e., a smaller size of amorphous interlayers between crystallites along the draw axis, which is calculated as the difference between L and l_{001} . All of the above structural features of cold-drawn films agree with the acoustic data (Fig. 4). As the draw ratio of the unloaded films is increased, one may only observe a slight increase in the speed of sound along the draw axis. The c axis of the lattice formed by the microfibrillar crystals is oriented parallel to the draw direction. This direction of the lattice is characterized by the highest modulus. As a result, a slight increase in the speed of sound is due to the fact that disassembling of lamellar crystals at low temperatures is not accompanied by their complete recrystallization upon the formation of microfibrillar crystals. Along with these crystals, a large amount of the anisotropic amorphous phase is formed, which exhibits intense molecular mobility at the given draw temperature. It is the increase in the proportion of this phase that may be responsible for the slight increase in the speed of sound with increasing cold-draw ratio (Fig. 4) and a substantial increase in the volume of the deformed film ΔV/V, which can be as high as 0.25.

Table 3. Changes in the spectral characteristics of cold-drawn films (T_d = 20□C, λ□= 4) under mechanical stress

ε, %	D/d,cm^{-1}	R	D/d,cm^{-1}	R	D/d,cm^{-1}	R
	410 cm^{-1}		442 cm^{-1}		70 cm^{-1}	
0	54	2.9	51	4.6	32	2.6
8	46	1.8	61	7.0	70	6.4

A significant increase in the speed of sound (acoustic modulus) upon the loading of the test film in the direction of the draw axis (curves 2, 3, Fig. 4) can be attributed only to a reversible transformation of the anisotropic amorphous (mesomorphic) phase to the crystalline state. A prerequisite for this transition is the increased density of the anisotropic phase, whose chains have the same conformation as the crystal into which they transfer.

This conclusion can be independently supported by the data presented in Table 3, which shows the spectral characteristics of some structurally sensitive IR absorption bands [6]. Three absorption bands were selected, of which one (at 410 cm^{-1}) is typical of the $TGTG^-$ chain conformation and the two other bands (442 and 70 cm^{-1}) correspond to the all-trans conformation [6]. As follows from Table 3, the normalized intensity (D/d) and dichroic ratio R of the first absorption band decrease upon loading. However, these parameters for the absorption bands at 442 and 70 cm^{-1} tend to rise. This implies that the conformational transitions $TGTG^- \rightarrow (TT)_n$ take place upon deformation of the cold-drawn films along the draw direction, with isomers with a helical conformation along the tensile draw axis being primarily involved. The 70-cm^{-1} band corresponds to vibrations in the lattice containing chains in the all-trans planar zigzag conformation [6]; hence, a strong increase in D/d and R (more than two times) in this case indicates that part of the amorphous-phase chains is additionally built in the crystal upon loading. This behavior is, most likely, common for all crystallizable polymers because a quite similar situation has been observed in the case of PET [23].

Thus, with increasing the draw ratio, the proportion of the anisotropic amorphous phase in the microstructure of the films must increase. If the (α_a-β)-process is associated with the regions of this phase, the significant increase in the enthalpy of activation of this relaxation region becomes understandable. The specific features of the morphology induced by cold drawing may also qualitatively explain the experimentally observed strong increase in the entropy of activation with increasing draw ratio (Table 1). The probability of formation of taut tie chains is known to increase in this case. For a small size of amorphous interlayers (Table 2) between neighboring crystals (acting as repulsive walls for kinetic segments), the tie chains have a low conformational entropy. Its additional decrease may be due to the presence of skewed crystallites in the cold-drawn films, as judged from the small-angle X-ray diffraction patterns (Table 2).

Certain information on the structural changes upon cold drawing may be obtained from the temperature dependences of relaxation strength $\Delta\varepsilon = \varepsilon_0 - \varepsilon_\infty$ of the above processes (Fig. 7). It is seen that a marked change in the slope of the curves takes place in the glass transition region. In the case of PE, the temperature dependence of the relative deformation of the excited segments of macromolecules displayed specific temperature points which were associated with an abrupt increase in the contribution of certain vibrational modes to internal energy [24]. Analysis shows that the increase in the deformation buildup rate at these points corresponds to the region of the emergence of a certain mobility type. As was shown earlier for another class of flexible-chain polymers (poly(alkylene oxide)s), certain vibrations in the segments of macromolecules impede the appearance of micro-Brownian motion in the amorphous regions upon the glass transition. The same situation may take place in the polymers studied in this work. Then, the low-temperature bending point in the Δε(T) plots in Fig. 7 corresponds to the excitation of certain vibrational modes in the polymer backbone. As a result, the free volume can strongly increase, thus creating the micro-Brownian cooperative mobility.

In the case of oriented films, the dielectric permittivity becomes anisotropic. When the draw direction corresponds to axis 1 and the normal to the film plane corresponds to axis 3 in the coordinate system, the ε* components indexed by 33 can be measured if the electrodes have been deposited in the given manner.Therefore, strictly speaking, Fig. 1 deals with ε''_{33} and Fig. 7 shows $\Delta\varepsilon_{33}$. The use of the Frelich formula for the relaxation strength in oriented films leads to the following expression [26, 27]:

$$\Delta\varepsilon = \Delta\varepsilon_{33} = \xi \frac{4\pi n}{3kT} \mu_e^2 \cos^2\gamma , \qquad (1)$$

where ξ is the factor of the local field, n is the concentration of dipoles with the effective dipole moment μ_e, and γ is the angle between the direction of the dipole moment and external electric field. Assuming that the dipole moment of the kinetic unit is perpendicular to the chain axis (a fragment in the all-trans conformation) and ignoring the contribution of anisotropy to the local field, we may represent Eq. (1) as [26]

$$\Delta\varepsilon = \xi \frac{\pi n}{3kT}[1+\langle\cos^2\theta\rangle]\mu_e^2 , \qquad (2)$$

(θ is the angle of disorientation of kinetic units). The aforementioned increase in Δε with increasing λ (Fig. 7) results from a change in three variables. Since the degree of crystallinity decreases upon cold drawing (see .. the values of normalized optical density at 470 cm^{-1} in Table 2 at draw ratios of 4 and 6), one of the factors is related to a concomitant increase in *n*. According to Eq. (2), a decrease in angle θ between the chain axis in the kinetic unit and draw direction (cf. the R_{470} values at different λ in Table 2) should also lead to an increase in Δε. An increase in λ upon cold drawing increases the proportion of all-trans conformation isomers [6]. These isomers are characterized by a higher lateral component of the dipole moment [6]; therefore, the μ_e values in the segments are higher at greater λ's. According to Eq. (2), this factor will also lead to an increase in Δε.

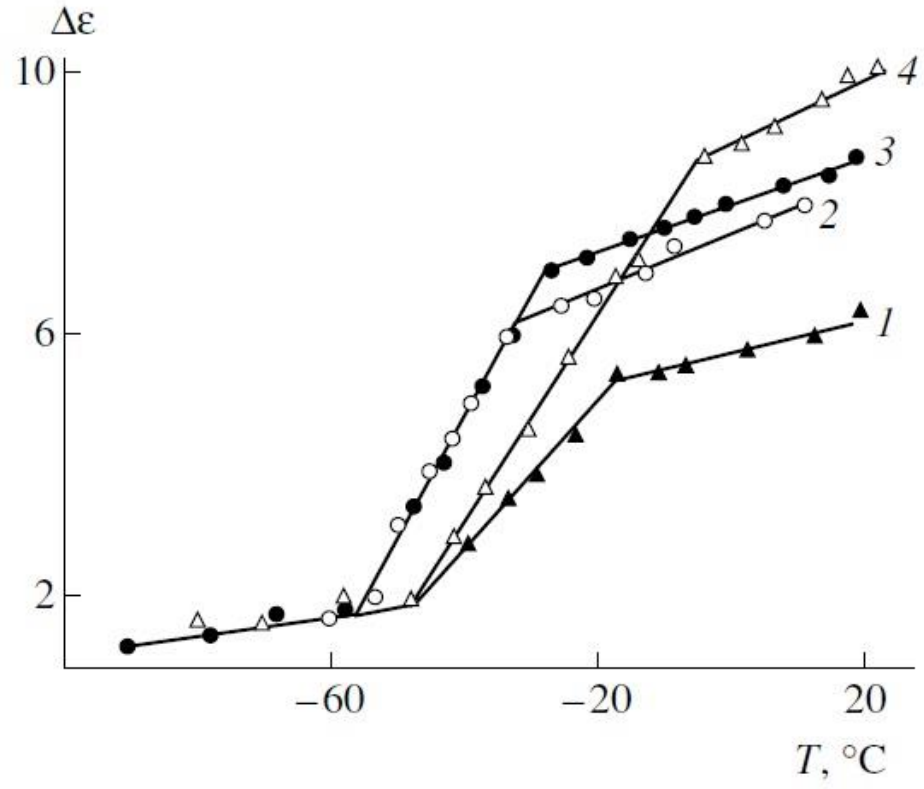

Fig. 7. The temperature dependences of relaxation strength in (*1*) the isotropic film and films with λ= (*2*) 2, (*3*) 4, and (*4*) 6.

Another aspect of the problem under consideration is the interpretation of the increase in Δε observed for all the samples with increasing the temperature (Fig. 7). For the temperature region above the glass transition point, this problem may be resolved to a certain extent using the data on the temperature dependence for in the small-angle X-ray reflection intensity in the VDF–HFP copolymer [28]. It was shown that cooling to below room temperature substantially decreases this intensity. If the intensity is proportional to (Δρ)2 , this finding implies that the density of the amorphous phase increases with approaching the glass transition point. Since the small-angle reflection intensity at the glass transition temperature is almost zero [28], the packing density in the disordered phase becomes comparable to that in the crystal. This situation may be reasonably explained if the disordered phase is assumed to exist primarily in the mesomorphic state [12]. When the temperature in the glass transition region is lowered, a transition (for example, of the nematic → crystal type) can take place in this phase and the heterogeneity in the electron density disappears. In this connection, the increase in Δε with increasing temperature (Fig. 7) should be related, according to Eq. (2), to an increase in μ_e due to the weakening of the interchain interaction.

ISSN: 0975-8585

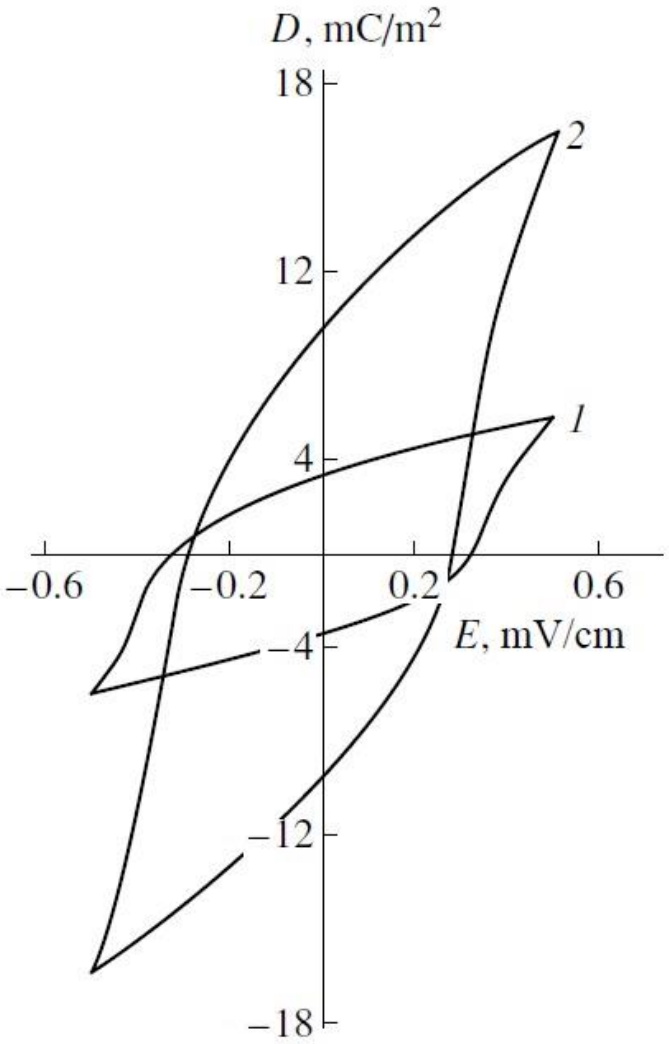

Fig. 8. Electric hysteresis curves for the ferroelectric films of the VDF–TFE copolymer under polarization at ambient conditions for (*1*) the isotropic film and (*2*) the cold-drawn film with λ⍰= 5.

CONCLUSION

Let us consider the effect of changes in the texture upon cold drawing on the ferroelectric characteristics of the copolymer. For this purpose, we compare dielectric hysteresis curves for the isotropic and cold-drawn samples under identical polarization conditions (T_p = 20°C, E_m = 500 kV/cm) (Fig. 8). As is seen, they differ in the values of residual P_r and spontaneous (maximum) P_s polarization. For the cold-drawn film, these quantities appear to be three times higher. If ferroelectricity for this class of compounds is assumed to be primarily dipolar in character [3], the P_r and P_s values measured are defined by P‹cos γ›, where averaging is performed over all dipoles. Taking into account that the dipole moment is perpendicular to the chain axis in our case [6], ‹cos γ› ~ ‹cos θ›. For the isotropic film, ‹cos θ› = 0.57; for the cold-drawn film, it is equal to 0.95, according to Table 2. Upon cold drawing, amorphization of the sample takes place and the number of polar crystals decreases. Therefore, the observed structural changes cannot explain the difference in P_r for the isotropic and oriented films. This conflict may be resolved by taking into account that reversible and irreversible changes in the degree of crystallinity occur in polymers when a strong field is applied [3, 6]. In the drawn samples under study, this process is quite feasible because of the increased amount of rotational isomers in the all-trans conformation in their anisotropic amorphous phase (see the normalized intensities of the absorption band at 470 cm^{-1}, Table 2). The placing of part of the chains in the anisotropic amorphous

phase with an increased packing density up to the crystal under the action of an external field does not require energy consumption because the ferroelectric crystal has chains of the same conformation [6]. The probability of these processes increases by virtue of the fact that, in the mesomorphic phase localized at the boundaries to the crystal, the mobility with reorientation frequencies of 10^6–10^7 s^{-1} (Fig. 2) is actualized at the polarization temperature. The generation of fluctuations in the orientations of the dipole moment of kinetic units by such motions in the presence of an applied field is responsible for the above increase in the degree of crystallinity under polarization.

ACKNOWLEDGMENTS

The article was prepared within the framework of the Federal Target Program (FTP) «Research and development on priority directions of development of scientific-technological complex of Russia for 2014-2020». The number of Agreements for the provision of grants: 14.576.21.0029, the unique project code: RFMEFI57614X0029.

REFERENCES

[1] Sawatari, C., Matsuo, M. Dependence of Thermal Crystallization of Poly(ethylene Terephthalate) on Active Mobility of Amorphous Chain Segments (1985) Textile Research Journal, 55 (9), pp. 547-555.

[2] Cais, R.E., Kometani, J.M. Structural studies of vinylidene fluoride-tetrafluoroethylene copolymers by nuclear magnetic resonance spectroscopy (1986) Analytica Chimica Acta, 189 (C), pp. 101-116.

[3] Kochervinskii, V.V., Glukhov, V.A., Sokolov, V.G., Romadin, V.F., Ostrovskii, B.I., Kuznetsova, S.Yu. (1989) Vysokomol. Soedin., Ser. A, 31 (11).

[4] Kochervinskij, V.V. Effect of the texture character and phase composition of polyvinylidene fluoride films on their ferroelectrical characteristics (1991) Vysokomolekularnye Soedineniya. Seriya A, 33 (10), pp. 2106-2114.

[5] Kochervinskij, V.V., Murasheva, E.M. Microstructure and ferroelectric properties of copolymers of vinylidene fluoride with tetrafluoroethylene of the 71/29 composition (1991) Vysokomolekularnye Soedineniya. Seriya A, 33 (10), pp. 2096-2105.

[6] Kochervinskii, V.V. The properties and applications of fluorine-containing polymer films with piezo- and pyro-activity (1994) Russian Chemical Reviews, 63 (4), pp. 367-371.

[7] Kochervinskij, V.V., Sokotov, V.G., Zubkov, V.M. Effect of the molecular structure on characteristics of electrical hysteresis of polyvinylidene fluoride and its copolymers (1991) Vysokomolekularnye Soedineniya. Seriya A, 33 (3), pp. 530-537.

[8] Kochervinskii, V.V., Malyshkina, I.A., Markin, G.V., Gavrilova, N.D., Bessonova, N.P. Dielectric relaxation in vinylidene fluorideHexafluoropropylene copolymers (2007) Journal of Applied Polymer Science, 105 (3), pp. 1101-1117.

[9] Kochervinskii, V.V., Kozlova, N.V., Khnykov, A.Y., Shcherbina, M.A., Sulyanov, S.N., Dembo, K.A. Features of structure formation and electrophysical properties of poly(vinylidene fluoride) crystalline ferroelectric polymers (2010) Journal of Applied Polymer Science, 116 (2), pp. 695-707.

[10] Kochervinskii, V.V., Kiselev, D.A., Malinkovich, M.D., Pavlov, A.S., Kozlova, N.V., Shmakova, N.A. Effect of the structure of a ferroelectric vinylidene fluoride- tetrafluoroethylene copolymer on the characteristics of a local piezoelectric response (2014) Polymer Science - Series A, 56 (1), pp. 48-62.

[11] Kochervinskii, V.V., Pavlov, A.S., Kozlova, N.V., Shmakova, N.A. Polarization of block textured films of ferroelectric copolymers of vinylidene fluoride with tetrafluoroethylene in an external field (2014) Polymer Science - Series A, 56 (5), pp. 587-602.

[12] Kochervinskii, V., Malyshkina, I., Pavlov, A., Pakuro, N., Bessonova, N., Shmakova, N., Bedin, S., Chubunova, E., Lebedinskii, Y. An effect of the electrode material on space charge relaxation in ferroelectric copolymers of vinylidene fluoride (2015) Journal of Applied Physics, 118 (24), art. no. 244102,

[13] Kochervinskii, V., Malyshkina, I., Pavlov, A., Bessonova, N., Korlyukov, A., Volkov, V., Kozlova, N., Shmakova, N. Influence of parameters of molecular mobility on formation of structure in ferroelectric vinylidene fluoride copolymers (2015) Journal of Applied Physics, 117 (21), art. no. 214101.

[14] Lagaron, J.M., Dixon, N.M., Reed, W., Pastor, J.M., Kip, B.J. Morphological characterisation of the crystalline structure of cold- drawn HDPE used as a model material for the environmental stress cracking (ESC) phenomenon (1999) Polymer, 40 (10), pp. 2569-2586.

[15] Waddon, A.J., Karttunen, N.R. Structural transitions during the cold drawing of aliphatic ketone terpolymers (2001) Polymer, 42 (5), pp. 2039-2044.
[16] Samon, J.M., Schultz, J.M., Hsiao, B.S. Study of the cold drawing of nylon 6 fiber by in-situ simultaneous small- and wide-angle X-ray scattering techniques (2000) Polymer, 41 (6), pp. 2169-2182.
[17] Takahashi, Y., Kodama, H., Nakamura, M., Furukawa, T., Date, M. Antiferroelectric-like behavior of vinylidene fluoride/trifluoroethylene copolymers with low vinylidene fluoride content (1999) Polymer Journal, 31 (3), pp. 263-267.
[18] Lagarón, J.M., López-Quintana, S., Rodriguez-Cabello, J.C., Merino, J.C., Pastor, J.M. Comparative study of the crystalline morphology present in isotropic and uniaxially stretched 'conventional' and metallocene polyethylenes (2000) Polymer, 41 (8), pp. 2999-3010.
[19] Asano, T., Baltá Calleja, F.J., Flores, A., Tanigaki, M., Mina, M.F., Sawatari, C., Itagaki, H., Takahashi, H., Hatta, I. Crystallization of oriented amorphous poly(ethylene terephthalate) as revealed by X-ray diffraction and microhardness (1999) Polymer, 40 (23), pp. 6475-6484.
[20] Mahendrasingam, A., Martin, C., Fuller, W., Blundell, D.J., Oldman, R.J., MacKerron, D.H., Harvie, J.L., Riekel, C. Observation of a transient structure prior to strain-induced crystallization in poly(ethylene terephthalate) (2000) Polymer, 41 (3), pp. 1217-1221.
[21] Meunier, M., Quirke, N. Molecular modeling of electron trapping in polymer insulators (2000) Journal of Chemical Physics, 113 (1), pp. 369-376.
[22] Meunier, M., Quirke, N., Aslanides, A. Molecular modeling of electron traps in polymer insulators: Chemical defects and impurities (2001) Journal of Chemical Physics, 115 (6), pp. 2876-2881.
[23] Kolb, R., Wutz, C., Stribeck, N., Von Krosigk, G., Riekel, C. Investigation of secondary crystallization of polymers by means of microbeam X-ray scattering (2001) Polymer, 42 (12), pp. 5257-5266.
[24] Neidhöfer, M., Beaume, F., Ibos, L., Bernès, A., Lacabanne, C. Structural evolution of PVDF during storage or annealing (2004) Polymer, 45 (5), pp. 1679-1688.
[25] Danch, A. Effect of supermolecular structure changes on the glass transition of polymer (2001) Journal of Thermal Analysis and Calorimetry, 65 (2), pp. 525-535.
[26] Li, L., Twum, E.B., Li, X., McCord, E.F., Fox, P.A., Lyons, D.F., Rinaldi, P.L. 2D-NMR characterization of sequence distributions in the backbone of poly(vinylidene fluoride-co -tetrafluoroethylene) (2012) Macromolecules, 45 (24), pp. 9682-9696.
[27] Nitta, K.-H., Nomura, H. Stress-strain behavior of cold-drawn isotactic polypropylene subjected to various drawn histories (2014) Polymer (United Kingdom), 55 (25), pp. 6614-6622.
[28] Xia, W., Xu, Z., Zhang, Z., Li, H. Dielectric, piezoelectric and ferroelectric properties of a poly (vinylidene fluoride-co-trifluoroethylene) synthesized via a hydrogenation process (2013) Polymer (United Kingdom), 54 (1), pp. 440-446.